Computer simulation study of the closure relations in hard sphere fluids

R. Fantoni[a)]
Dipartimento di Fisica Teorica dell' Università and Istituto Nazionale di Fisica della Materia, Strada Costiera 11, 34014 Trieste, Italy

G. Pastore[b)]
Dipartimento di Fisica Teorica dell' Università and INFM DEMOCRITOS National Simulation Center, Strada Costiera 11, 34014 Trieste, Italy

(Received 19 February 2004; accepted 19 March 2004)

We study, using Monte Carlo simulations, the cavity and the bridge functions of various hard sphere fluids: one component system, equimolar additive, and nonadditive binary mixtures. In particular, we numerically check the assumption of local dependency of the bridge functions from the indirect correlation functions, on which most of the existing integral equation theories hinge. We find that this condition can be violated either in the region around the first and second neighbors shell, or inside the hard core, for the systems here considered. The violations manifest themselves clearly in the so-called Duh–Haymet plots of the bridge functions versus the indirect correlation functions and become amplified as the coupling of the system increases. © *2004 American Institute of Physics.* [DOI: 10.1063/1.1739392]

I. INTRODUCTION

A central problem in the theory of the static structure of classical liquids is to find a simple and efficient way to obtain the pair correlation functions from the interparticle forces in pairwise interacting fluids. Exact statistical mechanics[1,2] allows us to write the formal solution of such problems as the coupled set of equations:

$$1+h_{ij}(r)=\exp[-\beta\phi_{ij}(r)+h_{ij}(r)-c_{ij}(r)+B_{ij}(r)] \tag{1}$$

and

$$h_{ij}(r)=c_{ij}(r)+\sum_l \rho_l \int d\mathbf{r}' c_{il}(r')h_{lj}(|\mathbf{r}-\mathbf{r}'|), \tag{2}$$

where $h_{ij}(r)$ and $c_{ij}(r)$ are the (total) and direct correlation functions for atomic pairs of species i and j, ρ_l is the number density of the lth component and $\beta=1/kT$. The functions $B_{ij}(r)$, named bridge functions after their diagrammatic characterization[1] are *functionals* of the total correlation functions, i.e., their value at distance r depends on the values of all the correlation functions at all distances.

The basic difficulty with Eqs. (1) and (2) is that we do not have an explicit and computationally efficient relation between $B_{ij}(r)$ and the correlation functions, so we have to resort to approximations. The results of the last three decades of research have shown that it is possible to make progress by approximating the bridge functionals $B_{ij}(r)$ by *functions* of the indirect correlation functions $\gamma_{ij}(r)=h_{ij}(r)-c_{ij}(r)$ (approximate closures). Once we have an explicit form for $B_{ij}(\gamma_{ij}(r))$, the resulting integral Eqs. (1) and (2), although approximate, can provide excellent results for the static structure of liquids. Moreover, besides the original focus on the structural properties, in recent years interest has grown toward using approximate integral equations to obtain thermodynamics and the phase diagrams of liquids and liquid mixtures.[3]

In particular, Kjellander and Sarman[4] and Lee[5] have derived an approximate but useful formula for the chemical potential of a fluid requiring only the knowledge of the correlation functions at the thermodynamic state of interest. Their formula is based on two main approximations. The first is the same assumption from which integral equations are derived, i.e., that the bridge functions $B_{ij}(r)$ are local functions of the corresponding indirect correlation functions. The second stronger assumption is that the only dependence of the bridge functions from the thermodynamic state is through the indirect correlation functions. Thus, the functional dependence of $B_{ij}(\gamma_{ij})$ is the same for all the states.

In this paper we want to investigate via direct numerical computer simulation the two approximations.

Up to now, numerical studies of the bridge functions and of the accuracy of the local approximation have been limited to the case of one component systems[6,7] or electrolytic solutions.[8] We feel that two-component systems deserve more interest for many reasons: (i) there are strong indications that the approximate universality of the bridge functions[9] is not valid in multicomponent systems, (ii) the phase diagrams of multicomponent systems are richer and more interesting than those of pure fluids, and (iii) it turns out that modeling the bridge functions for multicomponent systems is much more difficult than for pure systems.

We have studied, through Monte Carlo simulation, the bridge functions of a few systems of nonadditive hard spheres (NAHS) mixtures, including the limiting cases of additive (AHS) mixtures and one component system. In particular we are interested in a direct check of the local hypothesis for the functional relations between bridge and correlation functions in binary mixtures. To this aim we use the so

a)Electronic mail: rfantoni@ts.infn.it
b)Electronic mail: pastore@ts.infn.it

called Duh–Haymet plots.[8] These are plots of the partial bridge functions B_{ij} as a function of the partial indirect correlation functions γ_{ij}.

The paper is organized as follows: In Sec. II we summarize the equations we used to evaluate the cavity correlation functions from which the bridge functions can be easily obtained and we provide the relevant technical details of the numerical calculations. In Sec. III we present and discuss our numerical results.

II. CALCULATION OF THE CAVITY AND BRIDGE FUNCTIONS

A. Theory

The binary NAHS system is a fluid made of hard spheres of two species. One specie, here named 1, with diameter R_{11} and number density ρ_1 and another specie (2) with diameter R_{22} and number density ρ_2, with a pair interaction potential that can be written as follows:

$$\phi_{ab}(r)=\begin{cases}\infty & r<R_{ab},\\ 0 & r>R_{ab},\end{cases} \tag{3}$$

where $R_{12}=(R_{11}+R_{22})/2+\alpha$, with α being the nonadditivity parameter. We will also study various special cases as the one component system, and the binary mixture of additive hard spheres (AHS) $\alpha=0$. We can rewrite Eq. (1) to obtain the partial bridge functions

$$B_{ab}(r)=\ln y_{ab}(r)-\gamma_{ab}(r), \tag{4}$$

where $y_{ab}(r)$ are the partial cavity functions

$$y_{ab}(r)=g_{ab}(r)\exp[\beta\phi_{ab}(r)]. \tag{5}$$

Here $g_{ij}(r)=1+h_{ij}(r)$ are the partial radial distribution functions. Notice that both the cavity functions and the indirect correlation functions are everywhere continuous, and so is the bridge.

In the region outside the hard cores, in a hard sphere (HS) system, the cavity correlation functions coincide with the pair distribution functions $g_{ij}(r)$. In order to determine the relationship between the partial bridge functions and the partial indirect correlation functions within the hard cores, we need to calculate the partial cavity functions. There are two distinct methods for calculating them:[6] the one which uses Henderson's equation[10] and the direct simulation method of Torrie and Patey.[11] We decided to use the first method which is accurate at small r.

For a binary mixture the like cavity functions can be obtained from the following canonical average:

$$\begin{aligned} y_{aa}(r_{1_a2_a}) &= \frac{Vz_a}{N_a}\overline{y}_{aa}(r_{1_a2_a})\\ &= \frac{Vz_a}{N_a}\left\langle \exp\left\{-\beta\left[\sum_{i_a>2}^{N_a+1}\phi_{aa}(r_{1_ai_a})\right.\right.\right.\\ &\quad \left.\left.\left.+\sum_{i_b=1}^{N_b}\phi_{ab}(r_{1_ai_b})\right]\right\}\right\rangle_{N_1,N_2,V,T}, \end{aligned} \tag{6}$$

where a, $b=1$, 2 with $b\neq a$, $r_{i_aj_b}$ is the distance between particle i of specie a and particle j of specie b, $z_a=\exp(\beta\mu_a)/\Lambda^3$ is the activity of specie a, μ_a its chemical potential, and Λ the de Broglie thermal wavelength, V is the volume, N_a the number of particles of specie a, so that the prefactor $Vz_a/N_a=\exp(\beta\mu_a^{\rm exc})$, where $\mu_a^{\rm exc}$ is the excess chemical potential of specie a. The notation $\langle\cdots\rangle_{N_1,N_2,V,T}$ indicates the canonical average at fixed number of particles, volume, and temperature.

So to calculate $\overline{y}_{aa}(r)$ we need to introduce in the system of N_a+N_b particles labeled $1_b,\ldots,N_b$, $2_a,\ldots,(N+1)_a$ a test particle 1_a placed a distance r from particle 2_a and calculate, at each Monte Carlo step, the interaction of this particle with all the particles of the system except particle 2_a.

We immediately realize that when $r=0$ we must have

$$\overline{y}_{aa}(0)=1, \tag{7}$$

since the configurations where particle 2_a overlaps with other particles of the system are forbidden. Moreover, by

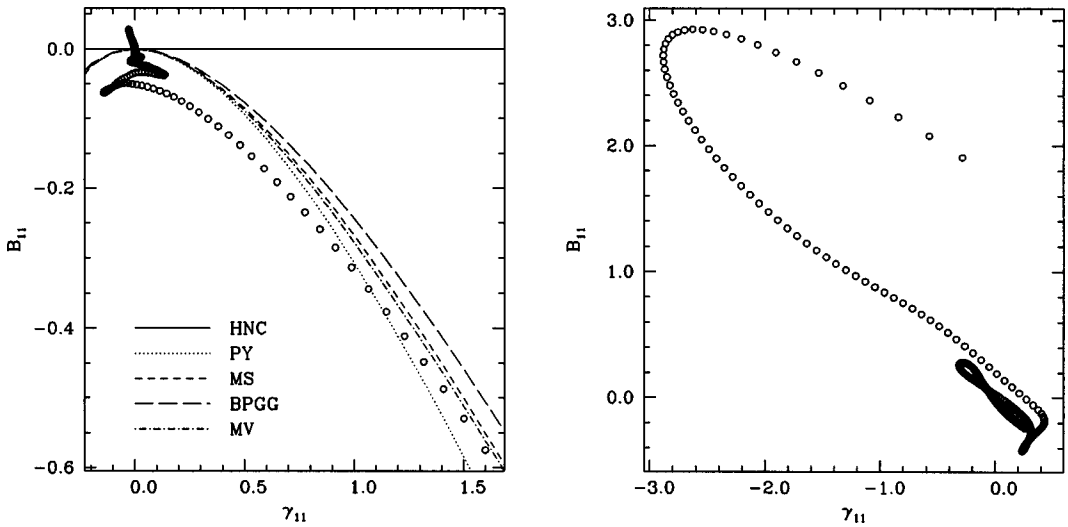

FIG. 1. The first two graphs are Duh–Haymet plots (dots), outside the hard core region, for the one component HS system (the lines show the behavior of integral equation closures). On the left $\rho=0.650$, on the right $\rho=0.925$.

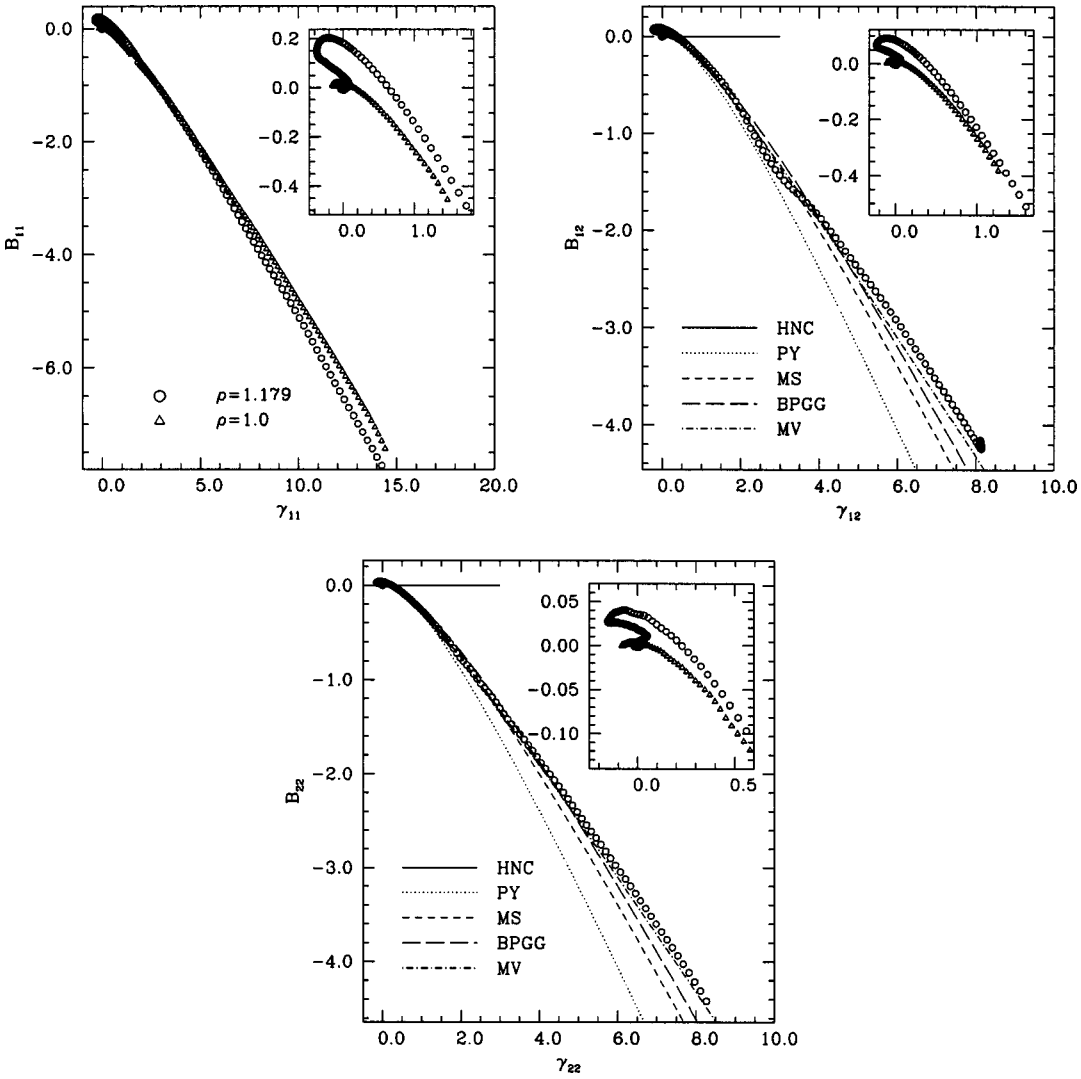

FIG. 2. Full Duh–Haymet plots obtained by the inversion of the Monte Carlo simulation data (dots) compared with some of the most common integral equation theories (lines) for the equimolar binary mixture of AHS at two different densities (in the second and third plot only results at the highest density are shown). $R_{11}=1$, $R_{12}=0.8$, and $R_{22}=0.6$. The insets shows the portion of the bridge function outside the hard cores.

taking into account that $y_{ab}(r)=g_{ab}(r)$ for $r>R_{ab}$ and from the asymptotic value of the partial pair distribution functions follows that

$$\lim_{r\to\infty} \overline{y}_{aa}(r)=e^{-\beta\mu_a^{\mathrm{exc}}}. \tag{8}$$

The unlike cavity functions can be obtained from the following canonical average:

$$y_{12}(r_{1_1 1_2})=\frac{Vz_1}{N_1}\overline{y}_{12}(r_{1_1 1_2})$$
$$=\frac{Vz_1}{N_1}\left\langle \exp\left\{-\beta\left[\sum_{i_2>1}^{N_2}\phi_{12}(r_{1_1 i_2})+\sum_{i_1>1}^{N_1+1}\phi_{11}(r_{1_1 i_1})\right]\right\}\right\rangle_{N_1,N_2,V,T}. \tag{9}$$

So to calculate $\overline{y}_{12}(r)$ we need to introduce in the system of N_1+N_2 particles labeled $1_2,\ldots,N_2$, $2_1,\ldots,(N+1)_1$ a test particle 1_1 placed a distance r from particle 1_2 and calculate, at each Monte Carlo step, the interaction of this particle with all the particles of the system except particle 1_2.

Now there is no simple argument to guess the contact value of $\overline{y}_{12}$. All we can say is that we must have $\overline{y}_{12}(0)\leqslant 1$. At large r we still have

$$\lim_{r\to\infty} \overline{y}_{12}(r)=e^{-\beta\mu_1^{\mathrm{exc}}}. \tag{10}$$

B. Numerical implementation

Monte Carlo simulations were performed with a standard NVT Metropolis algorithm[12] using $N=4000$ particles. Linked lists[12] have been used to reduce the computational cost. To calculate the partial pair distribution functions we generally used 5.2×10^8 Monte Carlo steps, where one step corresponds to the attempt to move a single randomly chosen particle, and incremented the histograms once every 20 $\times4000$ steps. To calculate the partial cavity functions we

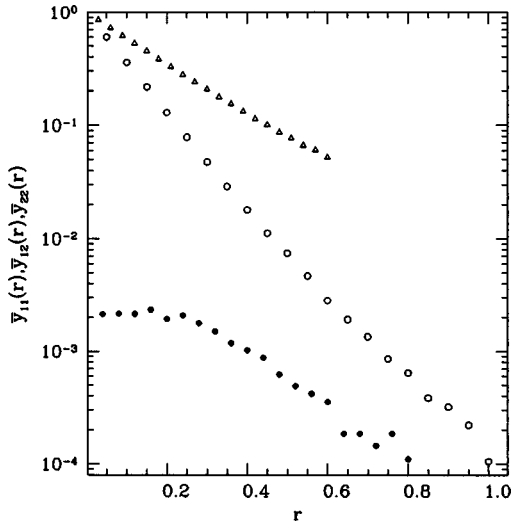

FIG. 3. Cavity functions inside the hard core for the equimolar binary mixture of AHS (at the same conditions as in Fig. 2 at the highest density). The plot shows the behavior of the functions defined in Eqs. (6) and (9) (notice the logarithmic scale on the ordinates), the triangles denote the 22 function, the open circles the 11 function, and the closed circle the 12 function.

used 1.6×10^9 Monte Carlo steps and incremented the histograms once every 2×4000 steps. The acceptance ratio was adjusted to values between 10% and 40%.

The Monte Carlo simulation returned the $g_{ab}(r)$ over a range not less than $8.125R_{11}$ for the densest system. In all the studied cases, the pair distribution functions attained their asymptotic value well inside the maximum distance they were evaluated. Thus, it has been possible to obtain accurate Fourier transforms of the total correlation functions $[\hat{h}_{ab}(k)]$ [it was necessary to cure the cusps at contact in the partial pair distribution functions by adding to them $H(R_{ab}-r)g_{ab}(R_{ab})$, H being the Heaviside step function, before taking the Fourier transform and removing its analytical Fourier transform afterwards]. To obtain the partial indirect correlation functions we first calculated the partial direct correlation functions $[\hat{c}_{ab}(k)]$ using the Fourier transform of the Ornstein–Zernike Eq. (2) and then we got the Fourier transform of the indirect correlation functions $\hat{\gamma}_{ij}(k)=\hat{h}_{ij}(k)-\hat{c}_{ij}(k)$ which is the transform of a continuous function in real space and then is safe to transform back numerically to obtain $\gamma_{ab}(r)$.

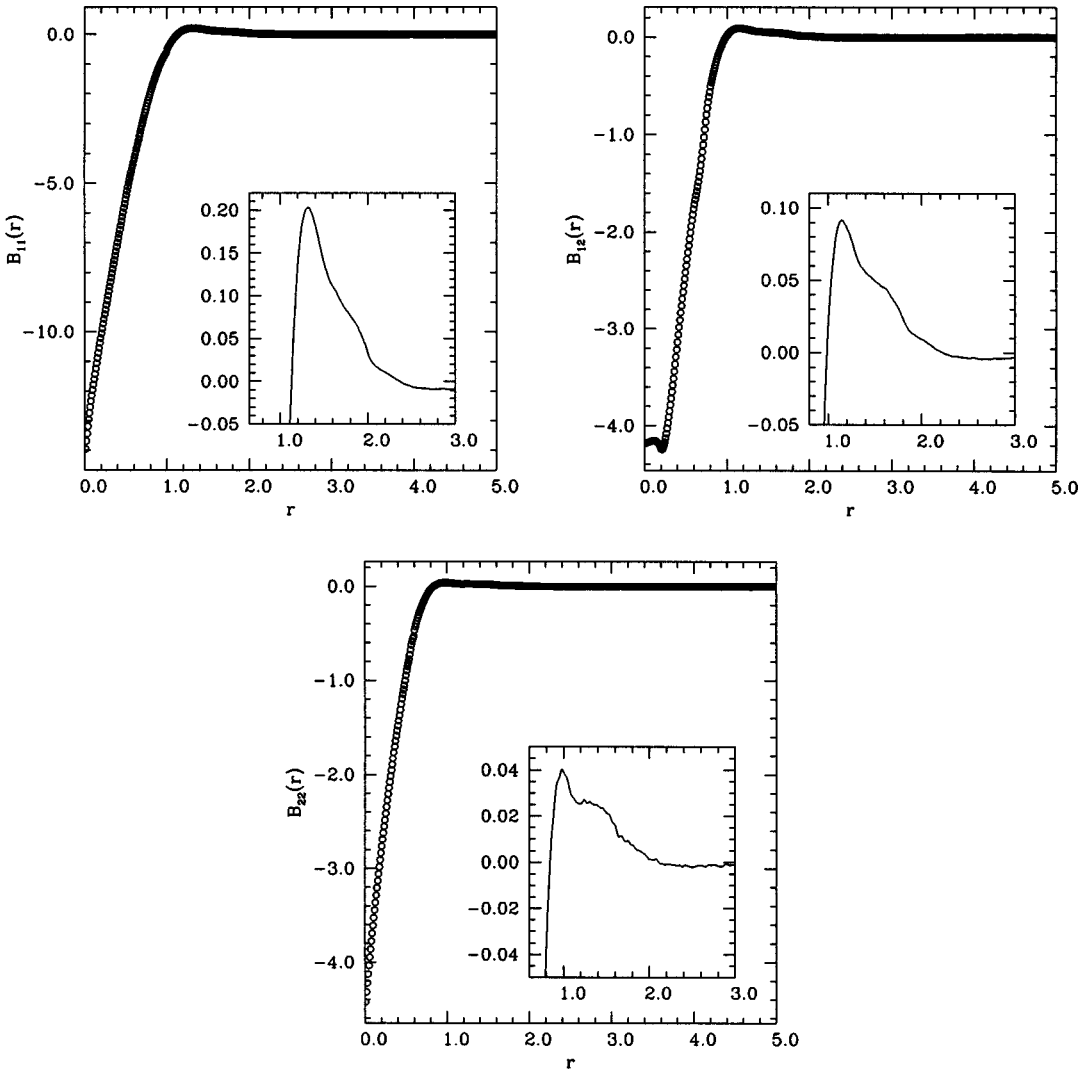

FIG. 4. Bridge functions $B_{ab}(r)$ for the equimolar binary mixture of AHS (at the same conditions as in Fig. 2 at the highest density). The insets shows magnifications of the regions just outside of the hard cores.

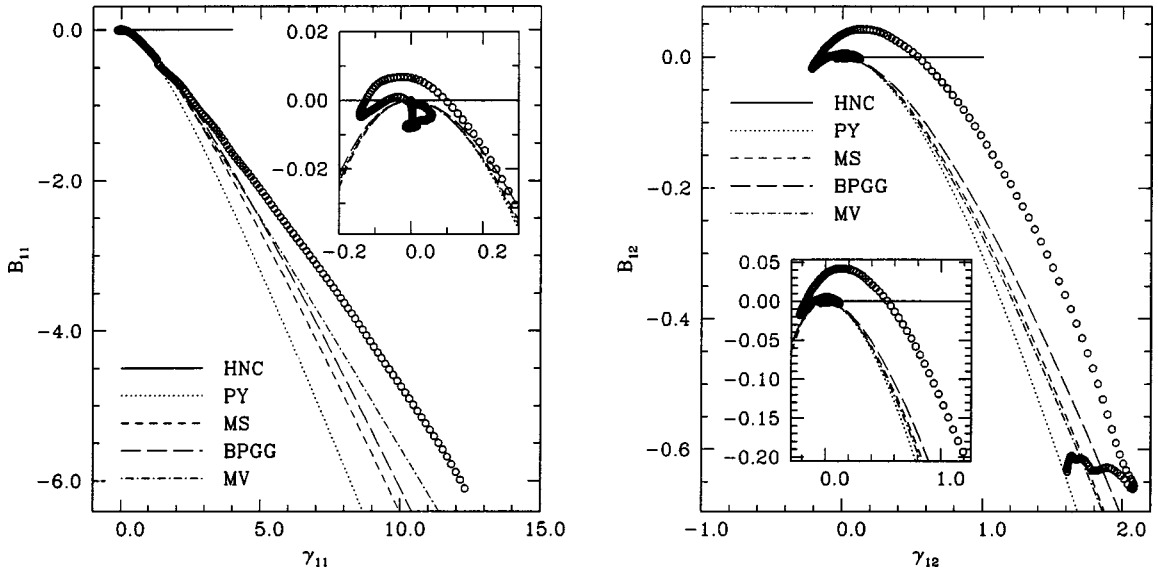

FIG. 5. Full Duh–Haymet plots obtained by the inversion of the Monte Carlo simulation data (dots) and by some of the most common integral equation theories (lines) for the equimolar binary mixture of NAHS with equal like diameters and negative nonadditivity $\alpha=-0.351$, at $\rho_1=0.589$. $R_{11}=R_{22}=1$ and $R_{12}=0.649$. The insets shows the portion of the bridge function outside the hard cores.

III. NUMERICAL RESULTS

We carried on simulations on the following systems: (A), one component HS; (B), equimolar binary mixture of AHS; (C), equimolar binary mixture of NAHS with equal like diameters and negative nonadditivity; (D), equimolar binary mixture of NAHS with equal like diameters and positive nonadditivity; and (E), equimolar binary mixture of NAHS with different like diameters. In all these cases we have drawn the corresponding Duh–Haymet plots, i.e., we plot, for each distance, the pairs $(B_{ij}(r),\gamma_{ij}(r))$.

When we are outside the hard core the partial bridge functions (4) reduces to

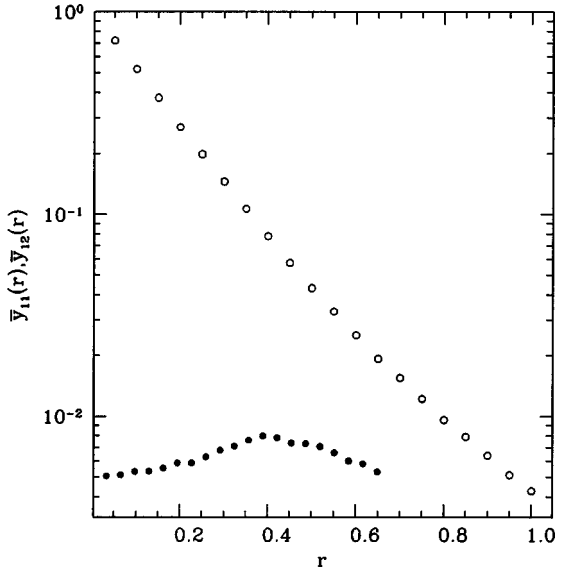

FIG. 6. Cavity functions for the equimolar binary mixture of NAHS with equal like diameters and negative nonadditivity (at the same conditions as in Fig. 5). The graph shows the behavior of the functions defined in Eqs. (6) and (9) (notice the logarithmic scale on the ordinates), the open circle denotes the like functions and the closed circle the unlike one.

$$B_{ab}(r)=\ln g_{ab}(r)-\gamma_{ab}(r) \tag{11}$$

and we can obtain the bridge functions directly from the pair correlation functions solving the OZ Eq. (2) to get the partial indirect correlation functions γ_{ab}.

To realize the Duh–Haymet plots when we are within the hard core regions, we first calculated the cavity functions $\overline{y_{ab}}$ as explained in Sec. II and then the bridge functions (up to an additive constant, the excess chemical potential $\beta\mu_a^{\mathrm{exc}}$) from their definition (4). Estimating the excess chemical potential from the long range behavior of the cavity functions [see Eqs. (8) and (10)] we were able to find the full bridge functions. Since the cavity functions in proximity of R_{ab} becomes very small, they are subject to statistical errors. In order to obtain smooth Duh–Haymet plots we needed to smooth the cavity functions obtained from the simulation. We did this by constructing the cubic smoothing spline which has as small a second derivative as possible.

A. One component HS

We carried out two simulations at $\rho_1\simeq 0.650$ (with a packing fraction of $\eta=\pi\rho_1 R_{11}^3/6=0.340$) and $\rho_1\simeq 0.925$ ($\eta=0.484$), the former corresponding to an intermediate density case and the latter to a liquid close to the freezing point. In our simulations we use R_{11} as a unit of length.

Inside the hard core, the bridge and the indirect correlation functions are monotonic and, for the cases here considered, there are no nonlocalities in the Duh–Haymet plots inside the core. Thus, to search for nonlocalities it is enough to analyze results in the external region. The resulting curves in the (B,γ) plane corresponding to points outside the hard core region are shown in Fig. 1. On the left the intermediate density case and on the right the high density one. We see that, as the density increases, the nonlocality becomes more accentuated. Of course, the quality of a local approximation does depend on the choice of the correlation functions used

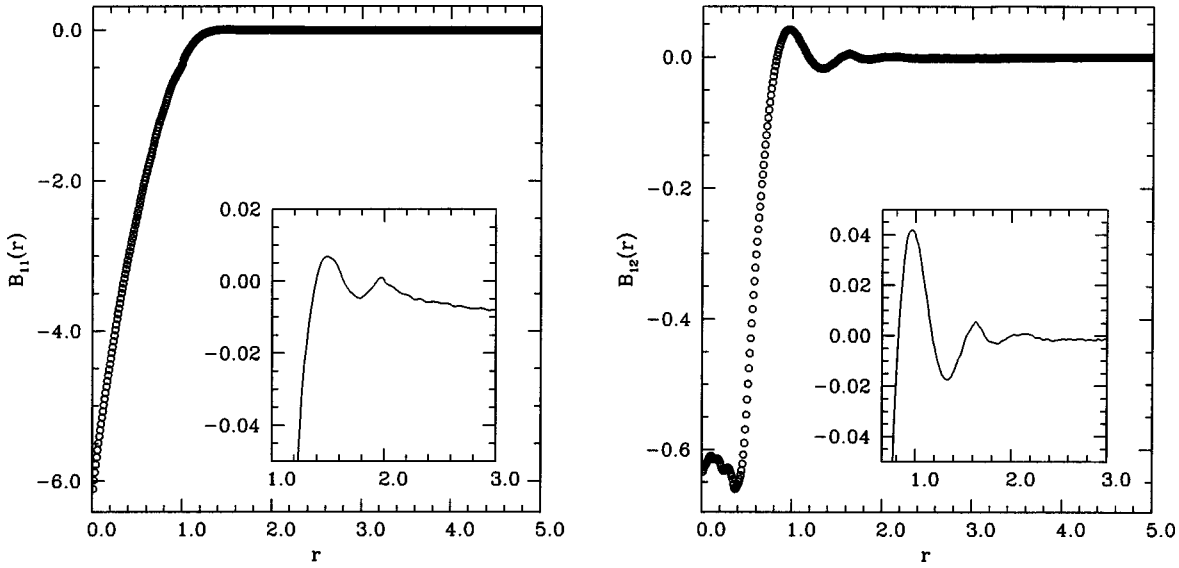

FIG. 7. Bridge functions $B_{ab}(r)$ for the equimolar binary mixture of NAHS with equal like diameters and negative nonadditivity (at the same conditions as in Fig. 5). The insets shows magnifications of the regions just outside of the hard cores.

as independent variable: plotting the bridge function as a function of the direct correlation function we observed the opposite behavior.

In order to compare the computer simulation results with the local approximate $B(\gamma)$ relations used in the integral equations, we have plotted the curves corresponding to different closures: the hypernetted chain (HNC):[1]

$$B(\gamma)=0, \tag{12}$$

the Percus–Yevick (PY):[1]

$$B(\gamma)=\log(1+\gamma)-\gamma, \tag{13}$$

the Martynov Sarkisov (MS),[13] and its generalization by Ballone, Pastore, Galli, and Gazzillo (BPGG):[14]

$$B(\gamma)=(1+\alpha\gamma)^{1/\alpha}-\gamma-1, \tag{14}$$

(MS) corresponds to $\alpha=2$, in the BPGG generalization α could be used as state dependent parameter to enforce thermodynamic consistence, here a fixed value of 15/8 has been used as suggested in (Ref. 14), and the modified Verlet (MV):[15]

$$B(\gamma)=\frac{-\gamma^2}{2[1+0.8\gamma]}. \tag{15}$$

We can see that the best closures (MS, BPGG, and MV), although not passing through the simulation curve, tend to follow its slope and curvature. When looking at Fig. 1 one should also bear in mind that the values of the bridge func-

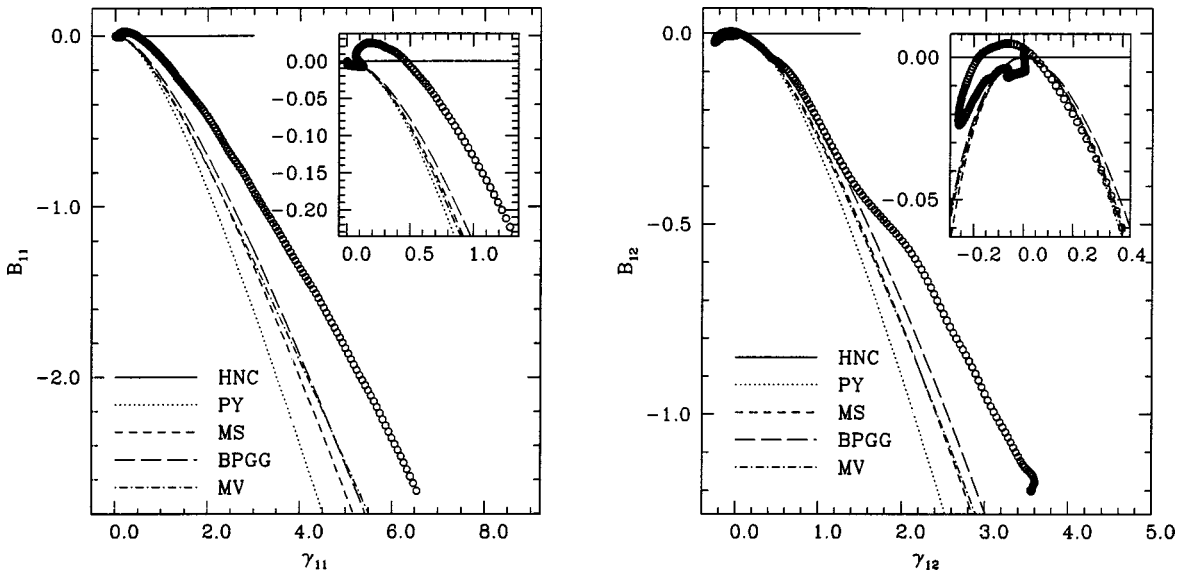

FIG. 8. Full Duh–Haymet plots obtained by the inversion of the Monte Carlo simulation data (dots) and by some of the most common integral equation theories (lines) for the equimolar binary mixture of NAHS with equal like diameters and positive nonadditivity $\alpha=+0.2$, at $\rho_1=0.200$. $R_{11}=R_{22}=1$ and $R_{12}=1.2$. The insets shows the portion of the bridge function outside the hard cores.

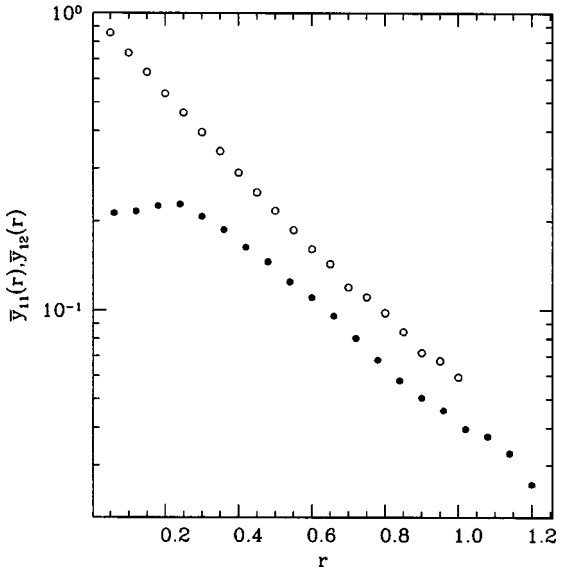

FIG. 9. Cavity functions for the equimolar binary mixture of NAHS with equal like diameters and positive nonadditivity (at the same conditions as in Fig. 8). The graph shows the behavior of the functions defined in Eqs. (6) and (9) (notice the logarithmic scale on the ordinates), the open circle denotes the like functions, and the closed circle the unlike functions.

tion outside the hard core are not the most relevant for the quality of the structural and thermodynamic results of the closures.

B. Equimolar binary mixture of AHS

We carried out a simulation at $\rho_1=\rho_2\simeq 0.589$ [$\eta=\pi(\rho_1 R_{11}^3+\rho_2 R_{22}^3)/6=0.375$] and $\rho_1=0.5$. We chose $R_{11}=1$, $R_{12}=0.8$, and $R_{22}=0.6$.

The results outside the hard core region are shown in the insets of the plots of Fig. 2. There are non-localities in a neighborhood of the origin which corresponds to the large r region. These are more evident in the high density case.

The most interesting feature shown in the figure is the difference between the curves at the two different densities. If the hypothesis of closures defined by a unique function $B(\gamma)$ would be exact data for different densities should collapse into a unique curve in these plots. The data shown in Figs. 1 and 2 indicate clearly that this is not strictly true. However, at low and intermediate densities the quantitative effect of the changing functional form is not dramatic. And even at the highest liquid densities, the success of closures such as MV, MS, or BPGG can be probably explained in term of a higher sensitivity of the theory to localized (near the contact) features of the bridge functions more than to the behavior over the whole range of distances.

Inside the hard core region the Duh–Haymet plots do not have nonlocalities. In Fig. 3 we show the results for the cavity functions $\bar{y}_{ab}$ for the system at the highest density. The plot for the unlike functions is more noisy than the plots for the like functions because $\bar{y}_{12}$ being smaller than $\bar{y}_{aa}$ for $a=1, 2$ is more subject to statistical error.

In Fig. 2 we show the full Duh–Haymet plots for the system at the highest density, from the simulation (dots) and from integral equation theories (lines). The plots show how the MV approximation is the best one for this system. The unlike bridge function starts at $r=0$ close to the MV approximation, stays close to this approximation as r increases and at some point have a smooth change in behavior and get closer to the PY curve.

Figure 4 shows the full bridge functions as a function of r for the system at the highest density. It is worth of notice the almost flat region of the unlike bridge near the origin.

C. Equimolar binary mixture of NAHS: $R_{11}=R_{22}$, $\alpha<0$

We carried out a simulation at $\rho_1=\rho_2\simeq 0.573$ ($\eta=0.6$). We chose $R_{11}=R_{22}=1$ and $R_{12}=0.649$ ($\alpha=-0.351$). These radii values would be suitable for a reference system to model correlation in molten NaCl.[16]

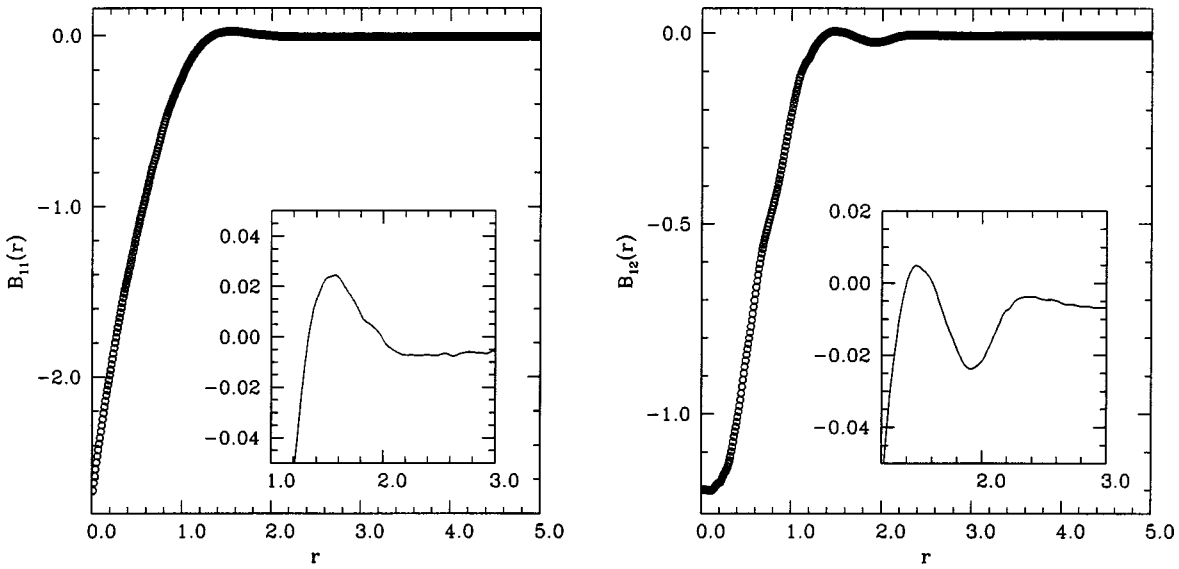

FIG. 10. Bridge functions $B_{ab}(r)$ for the equimolar binary mixture of NAHS with equal like diameters and positive nonadditivity (at the same conditions as in Fig. 8). The insets shows magnifications of the regions just outside of the hard cores.

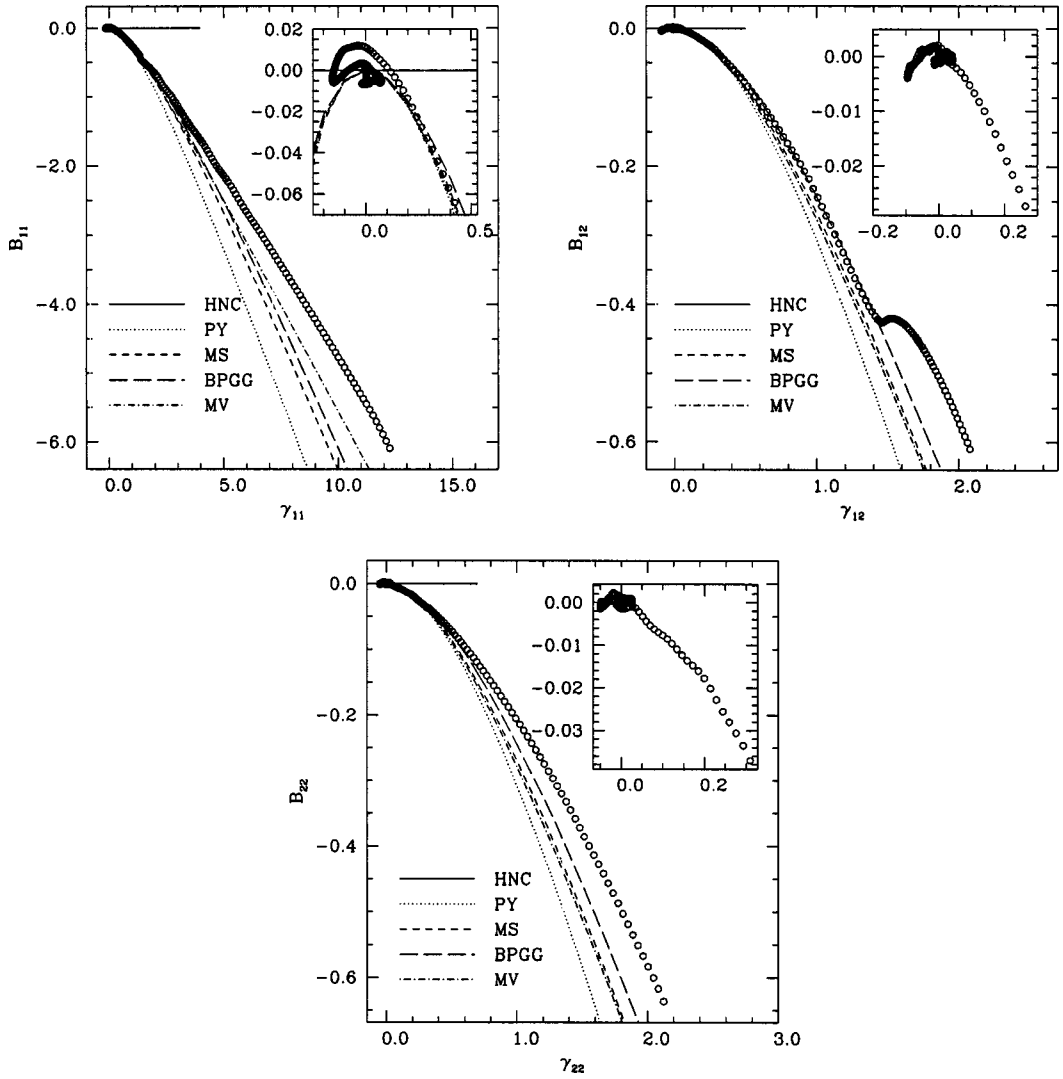

FIG. 11. Full Duh–Haymet plots obtained by the inversion of the Monte Carlo simulation data (dots) and by some of the most common integral equation theories (lines) for the equimolar binary mixture of NAHS with different like diameters $R_{11}=1$ and $R_{12}=R_{22}=0.6$, at $\rho_1=0.589$. The insets shows the portion of the bridge function outside the hard cores.

The results outside the hard core region are shown in the insets of the plots of Fig. 5. There are nonlocalities in the neighborhood of the origin corresponding to the large r region.

In Fig. 6 we show the results for the cavity functions $\bar{y}_{ab}$.

In Fig. 5 we show the full Duh–Haymet plots from the Monte Carlo simulation (dots) and from the most common integral equation theories (lines). The approximation which seems to be closer to the like bridge function is MV: only at big r the bridge functions is well approximated by PY, MS, BPGG, and MV. The unlike bridge function starts at $r=0$ close to the PY approximation but as r increases it has a sudden change in behavior which displaces it away from all the approximations. Inside the hard core region the Duh–Haymet plots for the unlike functions exhibit significant nonlocalities in correspondence with the non monotonic behavior of the unlike cavity function (black dots in Fig. 6).

Figure 7 shows the full bridge functions as a function of r. The unlike bridge function shows oscillations in a neighborhood of the origin.

D. Equimolar binary mixture of NAHS: $R_{11}=R_{22}$, $\alpha>0$

We carried out a simulation at $\rho_1=\rho_2\simeq 0.200$ ($\eta=0.209$). We chose $R_{11}=R_{22}=1$ and $R_{12}=1.2$ ($\alpha=+0.2$). Notice that this system undergoes phase separation when $\rho=2\rho_1>0.42$.

The results outside the hard core region are shown in the insets of the plots of Fig. 8. There are nonlocalities in a neighborhood of the origin corresponding to large distances.

Also for this system, inside the hard core region the Duh–Haymet plots for the unlike functions have nonlocalities in a neighborhood of $r=0$. These are smaller in extent than the ones found for system C. In Fig. 9 we show the results for the cavity functions $\bar{y}_{ab}$.

In Fig. 8 we show the full Duh–Haymet plots from the simulation (dots) and from the most common integral equa-

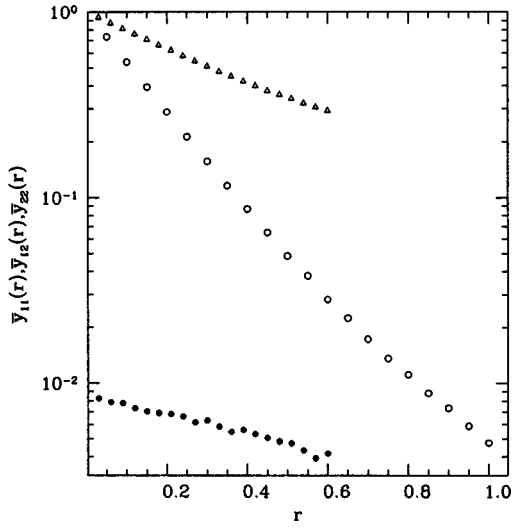

FIG. 12. Cavity functions for the equimolar binary mixture of NAHS with different like diameters (at the same conditions as in Fig. 11). The graph shows the behavior of the functions defined in Eqs. (6) and (9) (notice the logarithmic scale on the ordinates), the triangles denote the 22 function, the open circles the 11 function, and the closed circle the 12 function.

tions (lines). The approximations which seem to be closer to the like bridge function is MV and BPGG even if there is always a gap between the approximations and the simulation. The unlike bridge function starts at $r=0$ far away from all the approximations but as r increases it has a smooth change in behavior approaching the BPGG curve.

Figure 10 shows the full bridge functions as a function of r. Again, the unlike bridge function have an almost flat behavior in a neighborhood of the origin.

E. Equimolar binary mixture of NAHS: $R_{11} \neq R_{22}$

We carried out a simulation at $\rho_1=\rho_2\simeq 0.589$ ($\eta=0.375$). We chose $R_{11}=1$ and $R_{12}=R_{22}=0.6$ ($\alpha=-0.2$).

The results outside the hard core region are shown in the insets of the plots of Fig. 11. There are nonlocalities in a neighborhood of the origin which corresponds to the big r region.

Inside the hard core region the Duh–Haymet plots have no nonlocalities. In Fig. 12 we show the results for the cavity functions $\bar{y}_{ab}$.

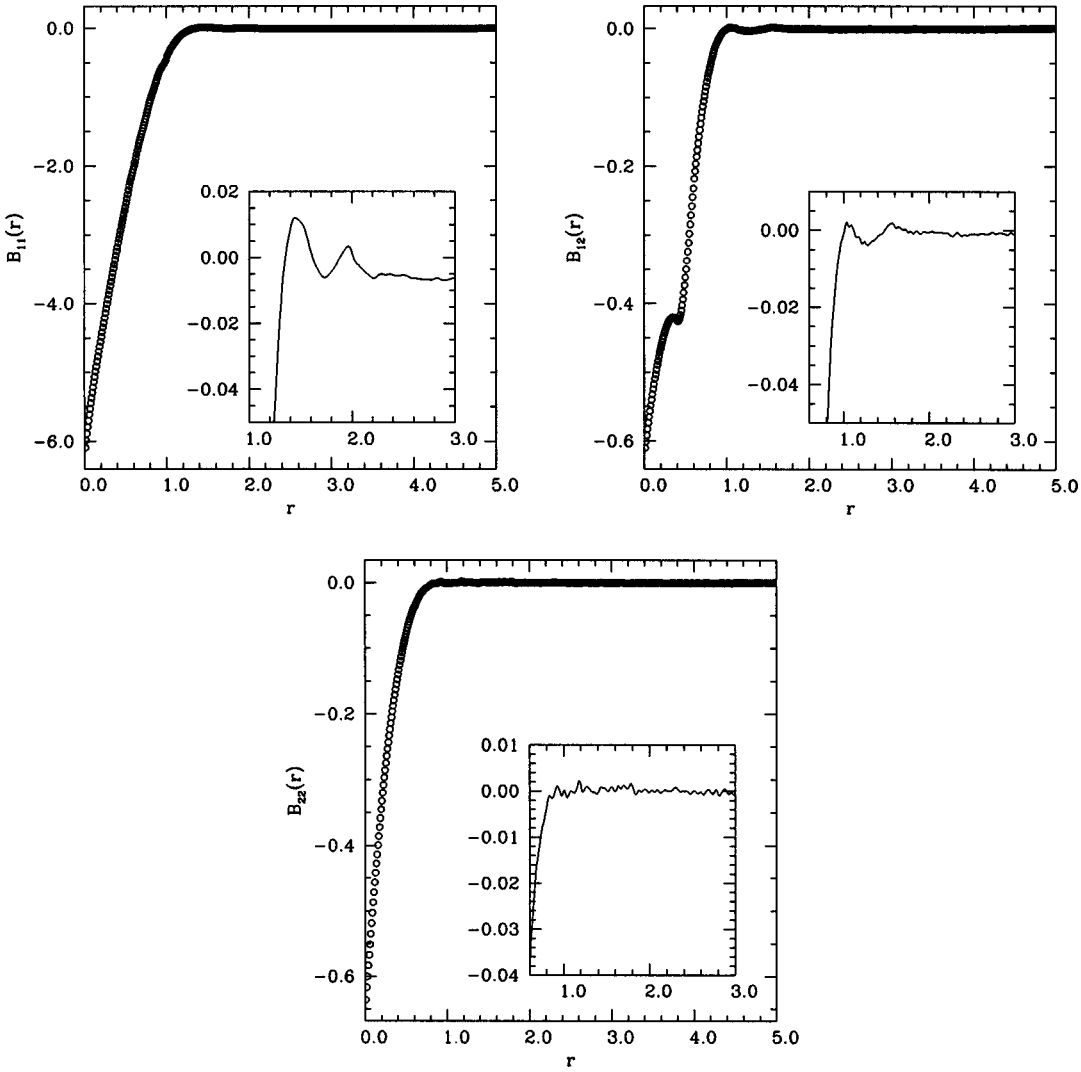

FIG. 13. Bridge functions $B_{ab}(r)$ for the equimolar binary mixture of NAHS with different like diameters (at the same conditions as in Fig. 11). The insets shows magnifications of the regions just outside of the hard cores.

In Fig. 11 we show the full Duh–Haymet plots from the simulation (dots) and from the most common integral equations (lines). The approximation which is closer to the 11 bridge function is the MV. The one that is closer to the 22 bridge function is the BPGG. The 12 bridge function starts at $r=0$ far away from all the 5 approximations and as r increases has a sudden change in behavior and starts following the BPGG approximation.

Figure 13 shows the full bridge functions as a function of r. The unlike bridge function shows again a qualitatively different behavior near the origin.

IV. CONCLUSIONS

From our analysis it follows that the nonlocalities in the function relationship between the bridge functions and the indirect correlation functions may appear either outside of the hard core regions or inside of it. While the nonlocalities outside the hard core appear both in the like and in the unlike functions, the ones inside the hard core appear only in the unlike functions (see Fig. 5 and Fig. 8), for the systems that we have studied. Their appearance can be directly related to the peculiar behavior of the unlike cavity correlation function inside the hard core.

As is shown by a comparison of the plots of Fig. 1 and from Fig. 2 the nonlocalities become more accentuated as we increase the coupling (the density) of the system. Nonetheless Fig. 8 shows that the nonlocalities may appear even in a weakly coupled system (in this case symmetric NAHS with positive non additivity). Among the systems studied the one which presents the worst nonlocalities is the equimolar symmetric NAHS with negative nonadditivity (see Fig. 5). For this system the Duh–Haymet plot for the unlike bridge function is nonlocal both in the hard core region (in a neighborhood of $r=0$) and outside of it (at large r).

We can conclude that the two hypothesis of a local function approximation for the bridge functionals of the indirect correlation functions and the stronger hypothesis of unique functional form independent on the state, are not strictly supported by the numerical data. For the one component system, this finding is consistent with the observed density dependence of the bridge function reported in Ref. 17. We observe clear violations of both the assumptions increasing with the density. This negative statement should be somewhat mitigated by realizing that the violations of the locality, in the systems studied, are limited to the small and large distances regions. The latter, corresponding to the region of the fast vanishing of the bridge functions affect very little the thermodynamic and structural properties of the systems. The former are presumably more important for the level of thermodynamic consistence of the theory but have small effect on quality of the structural results. The well known success of closures like MS, BPGG, and MV supports such point of view.

From comparison with the simulation data in the cases we have studied, we conclude that the best approximations of the true hard sphere bridge functions are provided by the MV and BPGG even if, especially in the unlike bridge functions, there are a wide variety of characteristic behaviors which are not captured by any of the most popular integral equation approximations. In this respect, we feel that a final comment on the local functional approximation in the case of multicomponent systems is in order. Indeed, density functional theory allows to say that the bridge function B_{ij} should be a functional of all the pair correlation functions, not only the (i,j) one. Thus, we could have a function approximation $B_{ij}(\gamma_{11}(r),\gamma_{12}(r),\gamma_{22}(r))$ which would be local in space but not with respect to the components. At the best of our knowledge, up to now no attempt has been done to explore this additional freedom to improve the modeling of the bridge functions in multicomponent systems.

[1] J. P. Hansen and I. R. McDonald, *Theory of Simple Liquids*, 2nd ed. (Academic, London, 1986).
[2] J. Caillol, J. Phys. A **35**, 4189 (2002).
[3] C. Caccamo, Phys. Rep. **274**, 1 (1996).
[4] R. Kjellander and S. Sarman, J. Chem. Phys. **90**, 2768 (1989).
[5] L. L. Lee, J. Chem. Phys. **97**, 8606 (1992).
[6] M. Llano-Restrepo and W. G. Chapman, J. Chem. Phys. **97**, 2046 (1992).
[7] D.-M. Duh and A. D. J. Haymet, J. Chem. Phys. **103**, 2625 (1995).
[8] D.-M. Duh and A. D. J. Haymet, J. Chem. Phys. **97**, 7716 (1992).
[9] Y. Rosenfeld and N. W. Ashcroft, Phys. Rev. A **20**, 1208 (1979).
[10] J. R. Henderson, Mol. Phys. **48**, 389 (1983).
[11] G. Torrie and G. N. Patey, Mol. Phys. **34**, 1623 (1977).
[12] M. P. Allen and D. J. Tildesley, *Computer Simulation of Liquids* (Clarendon, Oxford, 1987).
[13] G. A. Martynov and G. N. Sarkisov, Mol. Phys. **49**, 1495 (1983).
[14] P. Ballone, G. Pastore, G. Galli, and D. Gazzillo, Mol. Phys. **59**, 275 (1986).
[15] L. Verlet, Mol. Phys. **41**, 183 (1980).
[16] P. Ballone, G. Pastore, and M. P. Tosi, J. Chem. Phys. **81**, 3174 (1984).
[17] A. Malijevsky and S. Labik, Mol. Phys. **60**, 663 (1987).